Shock Waves (1999) 9: 113–123

Shock Waves

Critical tube diameter for detonation transmission and critical initiation energy of spherical detonation

I. Sochet[1], T. Lamy[1], J. Brossard[1], C. Vaglio[2], R. Cayzac[2]

[1] Laboratoire Energétique – Explosion – Structure, 63 Avenue de Lattre-de-Tassigny, F-18020 Bourges Cedex, France
[2] GIAT Industries – DSAM/DT/BIA, Route de Guerry, F-18023 Bourges Cedex, France

Received 5 July 1997 / Accepted 13 July 1998

Abstract. Two experimental setups are used to study propagation and attenuation of blast waves. In the first one, the blast wave is generated by a spherical detonation, and in the second one, the blast wave is created by the diffraction of a planar detonation propagating in a tube. The similarity of these phenomena appears clearly by means of dimensionless space-time and pressure-space diagrams of shock wave propagation. Dimensionless variables are expressed as a function of the supplied energy. Two energy formulations are proposed: a piston model and a bulk energy model. The established diagrams cover a wide range of industrial applications. Under critical conditions, the energy released by a planar detonation is correlated to the ignition source energy supply and a relationship which links the critical radius of detonation to the critical tube diameter.

Key words: Propane, Hydrogen, Shock wave attenuation, Shock wave diffraction, Similarity law, Gaseous detonation, Explosion energy

1 Introduction

For engineering applications, it is important to predict the critical initiation energy of spherical detonation in gaseous mixtures. To simulate the above, two principal modes of initiation are available: a point source or a confined planar detonation wave transmission at the open end of a tube into an unconfined environment. In order to analyze these modes of initiation, two approaches are possible: the first one is experimental in which the critical initiation energy of a spherical detonation from a point energy deposition (exploding wire, solid explosive charge, etc ...), or from the critical tube diameter; these are independent modes and both are directly measurable. The second one is based on a phenomenological analysis and on the dynamic parameters of the detonable mixture. It produces various relationships which are dependent on the cell width. The object of this paper is to correlate these two types of initiation. To that end, it is necessary to express the energy deposited by each experimental device or to calculate this energy taking into account the characteristics of the detonable mixture. The first step is to compare the characteristic of propagation and attenuation of the shock waves generated by each mechanism to deduce nominal energy outputs and then to compare them with the calculated energies. Consequently, the relationship between the critical radius of detonation, R_{cCJ}, and the critical tube diameter, d_c, of detonation transmission will be deduced.

Correspondence to: I. Sochet
An abridged version of this paper was presented at the 16th Int. Colloquium on the Dynamics of Explosions and Reactive Systems at Krakow, Poland, from July 27 to August 1, 1997.

2 Explosion energy: phenomenological approach

In the case of a detonation tube, the energy supply can be expressed by the piston model or by the minimum surface energy model.

2.1 Piston model

The piston model defines the work done to the outside volume by a piston (interface separating the expanding combustion products from the tube with the gas originally in a larger volume) propagating at constant speed. Initially the planar detonation wave propagates in a constant cross sectional tube (diameter d) and emerges from the tube to the larger volume: the planar detonation wave transforms subsequently to a quasi-spherical wave. Consequently, the energy supply E is a function of time and given by:

$$E = \int_0^t pS(t)dt. \quad (1)$$

Now the difficulty is to obtain a numerical estimation of such an integration. Two methods are proposed.

From the concept of Matsui and Lee (1979), the local energy released by the planar Chapman-Jouguet detonation wave near the tube axis is effective (throughout $S(t)$) up to a time $t = (d/2)/a$ (where "a" is the speed of sound behind the detonation front) in the creation of the spherical wave:

$$E = \int_0^t p_{CJ} u_{CJ} \pi (a_{CJ} t)^2 dt,$$

thus

$$E_1 = \frac{\pi}{24} p_{CJ} \frac{u_{CJ}}{a_{CJ}} d^3. \quad (2)$$

In Desbordes (1988) the energy supply is integrated directly as $E(t) = p_b u_b S(t) t$, where $S = \pi (a_b t)^2$ and $t = (d/2)/a_b$,

$$E_2 = \frac{\pi}{8} p_b \frac{u_b}{a_b} d^3. \quad (3)$$

The subscript b denotes the state of burned gases concerning the overdriven detonation branch of the Hugoniot curve.

Equations (2) and (3) lead to following remarks:

(1) E_1 and E_2 approximate the energy required to initiate a spherical detonation. In fact, initially the created wave takes a hemispherical form. A factor of magnitude 2 has, therefore, been applied to allow for this effect and to compare the energy available by a detonation tube and a concentrated point source.
(2) The distance corresponding to the time while the deposition of energy is effective does not represent the point from which the wave becomes spherical. Effectively, the smaller the tube diameter is, the more the energy supply can be considered as concentrated on a point and the more the sphericity is obtained rapidly.
(3) E_1 and E_2 should be equal at the Chapman-Jouguet state; however, there is a factor of 3 between these two relations.

Here, the expressions of energy obtained by Matsui and Lee (1979) and Desbordes (1988) are generalized by the following equation,

$$E = K_1 p \frac{u}{a} d^3, \quad (4)$$

where K_1 is a constant to be determined analytically.

2.2 Surface energy model

The surface energy concept is based on the strong blast theory and defines the necessary minimum surface before a planar wave can evolve into a spherical wave without failure. Lee (1984) proposes to equate the surface energy of the blast wave to the area of the critical tube. The resultant expression of the critical energy is given by $E = 4\pi\gamma_0 p_0 M_{CJ}^2 I(\frac{d}{4})^3$, where I is the integral of dimensionless energy, which can be approximated by $I = E_v/(3\rho_0 D_{CJ}^2)$ in the case of a spherical wave, E_v denotes the chemical energy per unit volume released by the reaction. Substituting I into E yields,

$$E = \frac{\pi}{48} E_v d^3. \quad (5)$$

The energy expressed in this form is only applicable to a Chapman-Jouguet detonation wave (in the case of strong detonation, the factor $\pi/48$ is not valid). Here, we adopt the more general following form,

$$E = K_2 E_v d^3. \quad (6)$$

These two models must correspond to the same initiation energy. Consequently, for the Chapman-Jouguet condition (4) and (5) are equivalent:

$$K_1 p_{CJ} \frac{u_{CJ}}{a_{CJ}} d^3 = \frac{\pi}{48} E_v d^3 \quad \text{i.e.} \quad K_1 = \frac{\pi}{48} \frac{a_{CJ}}{u_{CJ}} \frac{E_v}{P_{CJ}}. \quad (7)$$

The numerical value of K_1 can be estimated by using the approached formulations defining thermodynamics characteristics at the Chapman-Jouguet state: $p_{CJ} \approx \rho_0 D_{CJ}^2/(\gamma_{CJ}+1)$ with $\gamma_{CJ} = 1.2$ and $D_{CJ}^2 = 2(\gamma_{CJ}^2 - 1)\Delta_R H^*$ where $\Delta_R H^*$ is the mass enthalpy of the reaction at standard state (*): $\Delta_R H^* = E_v/\rho_0$ and the subscript 0 defines the initial state. Hence, $p_{CJ} \approx 2E_v(\gamma_{CJ} - 1)$. Furthermore, $a_{CJ} = \gamma_{CJ} D_{CJ}/(\gamma_{CJ}+1)$ and $u_{CJ} = D_{CJ}/(\gamma_{CJ}+1)$. As a result, the constant K_1 can be evaluated as:

$$K_1 = \frac{\pi}{48} \frac{\gamma_{CJ}}{2(\gamma_{CJ}-1)} = \frac{\pi}{16}. \quad (8)$$

Hence, the energy should be effective on a distance shorter than for a supposed perfectly spherical symmetry.

From an experimental point of view, we have to establish dimensionless space-time (R, T) and pressure-space (P, R) diagrams relative to a spherical shock wave generated by either an explosion of sphere or a transmission of a planar detonation or shock wave emerging from a tube into an inert medium. If we refer to (4) available for different states described by dynamic adiabatics, the pressure (p), the particular absolute velocity (u), the sound speed (a) represent the gas state downstream of the wave. This wave can be a Chapman-Jouguet detonation wave, an overdriven detonation wave (in the case of a converging detonation tube), or a shock wave as we shall describe in the applications below. Variables p, u and a are calculated from the classical Hugoniot relationships. They are summarized in Table 1. With regard to the formulation of (6), the term E_v is given by: (i) either the chemical energy E_v per unit volume released by the thermochemical reaction; (ii) or the kinetic and internal energies of the gas bounded by the shock wave: $E_v = (\rho u^2/2) + (p/(\gamma - 1))$.

Hence, (6) can be applied to shock tubes, for example. Finally, leaving aside arguable constant K_i, the energy supply is written as follows:
in the case of a tube of diameter d:

$$E = K_1 p \frac{u}{a} d^3 \quad (9)$$

or

$$E = K_2 E_v d^3 \quad (10)$$

in the case of a sphere of initial radius R_0:

$$E = K_3 p \frac{u}{a} R_0^3 \quad (11)$$

Table 1. Rankine-Hugoniot relations through detonation wave and shock wave (p, pressure; u, absolute particle velocity; a, sound speed)

	p	u	a
Overdriven detonation $M \gg M_{CJ}$ $\gamma = 1.2$	$\frac{2\rho_0 D^2}{\gamma+1}$	$\frac{2D}{\gamma+1}$	$\frac{D[2\gamma(\gamma-1)]^{1/2}}{\gamma+1}$
Chapman-Jouguet detonation $\gamma_{CJ} = 1.2$	$\frac{\rho_0 D_{CJ}^2}{\gamma_{CJ}+1}$	$\frac{D_{CJ}}{\gamma_{CJ}+1}$	$\frac{\gamma_{CJ}}{\gamma_{CJ}+1} D_{CJ}$
Strong shock wave $M \gg 1$ $\gamma_0 = 1.4$	$\frac{2\rho_0 M_s^2}{\gamma_0+1} p_0$	$\frac{2D}{\gamma_0+1}$	$D\left(\frac{\gamma_0-1}{\gamma_0+1}\right)\left(\frac{2\gamma_0}{\gamma_0-1}\right)^{1/2}$
Shock wave $\gamma_0 = 1.4$	$\frac{2\gamma_0 M_s^2-(\gamma_0-1)}{\gamma_0+1} p_0$	$\frac{2D(M_s^2-1)}{(\gamma_0+1)M_s^2}$	$D\left[\frac{2+(\gamma_0-1)M_s^2}{(\gamma_0+1)M_s^2}\right]\left[\frac{2\gamma_0 M_s^2-(\gamma_0-1)}{(\gamma_0-1)M_s^2+2}\right]^{1/2}$

M_s, Mach number of shock wave; Subscripts: 0 initial conditions; CJ Chapman-Jouguet conditions

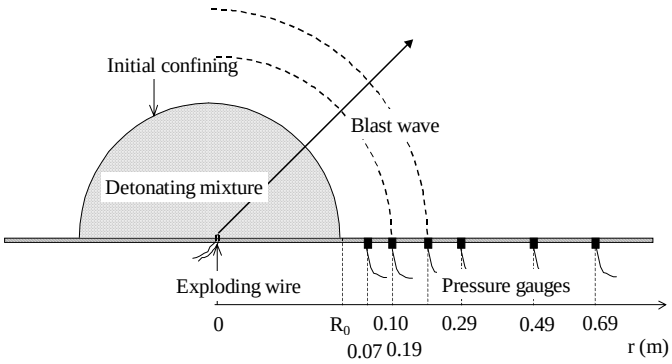

Fig. 1. Experimental configuration: hemispherical detonation

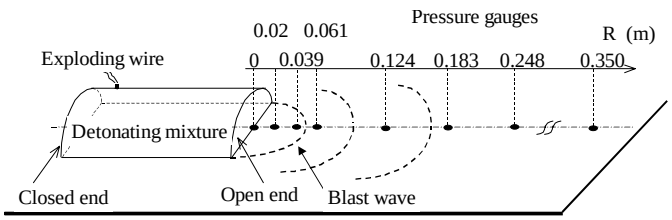

Fig. 2. Experimental configuration: half detonation tube

or

$$E = K_4 E_v R_0^3 . \tag{12}$$

Hence, these models are called "piston model" (9), (11) and "bulk energy model" (10), (12), respectively.

3 Experiment

The experimental investigation is based on small scale experiments. Two different experimental setups are used to obtain spherical shock waves: a point source and the transmission of a confined planar detonation wave at the open end of a tube into an unconfined environment. The first one (Fig. 1) represents an explosive gaseous charge confined in a hemispherical volume (Sochet et al. 1993). The initial radius R_0 varies from 40 mm to 80 mm. We have used propane-oxygen mixtures, C_3H_8+nO_2 (n = 3,4,5 and 7), and stoichiometric hydrogen-oxygen mixtures H_2/O_2. A spherical detonation was initiated by means of an exploding wire located at the center of symmetry at ground level. In the second (Fig. 2), the planar detonation propagates in a cylindrical half tube operating with the same gaseous mixtures (C_3H_8 + $3O_2$, C_3H_8 + $5O_2$, C_3H_8 + $7O_2$, H_2 + $0.5O_2$). The inner diameter d of the tube varies from 16 mm to 36 mm. The length is 400 mm. Some experiments were also performed with a convergent adaptor of a tube of 36 mm diameter. This convergence is characterized by a 31.5 mm length, a 36 mm enterance diameter and 16 mm open end diameter. Only the stoichiometric propane-oxygen mixture is used with the convergent section. The detonation is initiated at the closed end of the detonation tube by an exploding wire. The planar detonation wave propagates through an orifice generating a blast wave in the surrounding air. The measurements of shock wave parameters are conducted by pressure transducers (Kistler 603B) distributed on the plane: (i) at radial distances r from the explosion center ($1.75 \leqslant r/R_0 \leqslant 17$); and (ii) in the axis of the cylindrical half tube at radial distances r from the orifice ($0 \leqslant r/d \leqslant 22$).

4 Experimental results

4.1 Pressure records

Typical overpressure records for a blast wave generated by a detonation are presented in Figs. 3a and 3b.

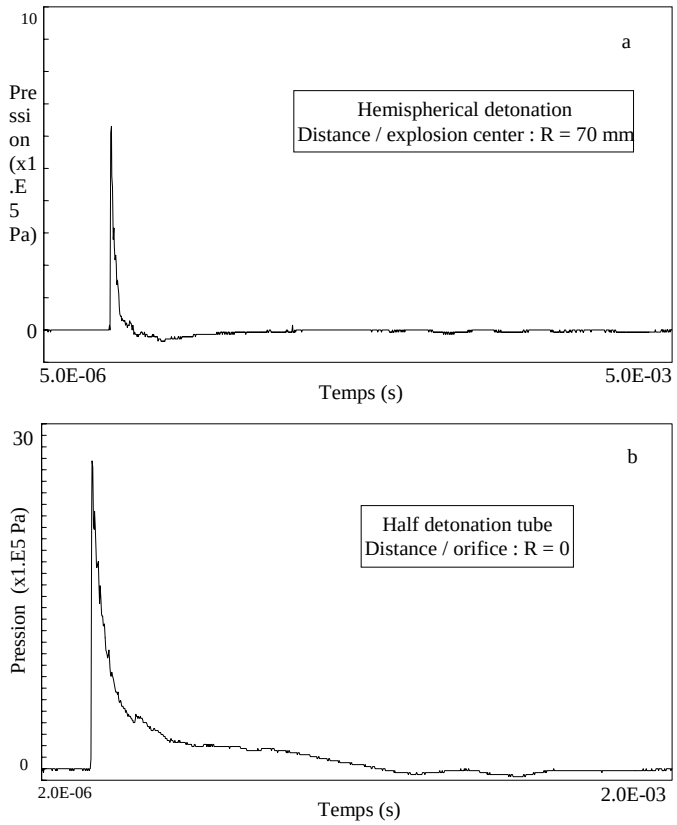

Fig. 3a,b. Incident static pressure: **a** point source; **b** detonation tube

For a point source (Fig. 3a), six parameters characterize the blast wave pressure profile: peak overpressure during the positive phase; positive phase duration; positive phase impulse; peak overpressure during the negative phase; negative phase duration; and negative phase impulse.

The pressure signal of the blast wave generated the detonation tube (Fig. 3b) shows at first pressure gauge located at the muzzle: characteristic pressure-peak whose amplitude is less than the ZND peak. At other gauges, there is a peak and a small positive phase impulse. There is no negative phase.

4.2 (r-t) and (p-r) diagram

For this study, two characteristics from pressure records are retained: shock arrival times (t) and peak pressure (p). Diagrams of shock wave which relate the radial distance r of the shock front time t on one hand, and those which relate the maximum pressure to the radial distance of the shock front on other hand, either a point source or a detonation tube, are established for a given initiation energy.

The diagrams $(r-t)$ (Figs. 4, 5) and $(p-r)$ (Figs. 6, 7) of shock wave are established for each of the cases: Figures 4 and 6 correspond to the point source while Figs. 5 and 7 detonation tube. Time and radial distance of the shock front scales relative to the point source are twice times as great as those relative to the detonation tube, whereas there is a factor 1/3 on pressure scale. Considering scales, the $(r-t)$ diagram brings out results more displayed in case of point source (Fig. 4) than detonation tube (Fig. 5). The envelop of curves gets wider with increasing radial distance from the source. For the point source case (Fig. 4), the hydrogen fuel has a wider band than the propane fuel. In detonation tube case (Fig. 5), the results are dependent on the tube diameter and independent of the gaseous mixture: as the diameter decreases the slope of curve decreases. The evolution of radius of shock front versus time is represented by a power law function $r = At^n$. Values of constants A and n are listed in Tables 2 and 3. Dispersal measurements are more important on $(p-r)$ diagrams (Figs. 6, 7). The envelop curves contract with increasing radial distance. It emerges from $(p-r)$ diagrams that maximum pressure of the shock front decreases too rapidly. In the far field, the wave propagates at sound speed at following coordinates: (i) $r \propto 600$ mm and $1 \times 10^{-3} \leq t(s) \leq 1.4 \times 10^{-3}$ for the point source; (ii)

Table 2. Point source $R(m) = A[t(s)]^n$: space-time diagrams coefficients of shock wave

Gaseous mixture	R_0 (mm)	A	n
		0.19 ≤r (m)≤ 0.69	
$C_3H8+3\ O_2$	50	56.345	0.676
$C_3H8+4\ O_2$	50	60.912	0.690
$C_3H8+5\ O_2$	50	62.828	0.694
$C_3H8+7\ O_2$	50	64.700	0.702
		0.07 ≤r (m)≤ 0.29	
$C_3H8+5\ O_2$	40	31.355	0.616
	50	27.680	0.592
	60	31.920	0.601
		0.07 ≤r (m)≤ 0.69	
$H_2+0.5O_2$	40	41.136	0.659
	50	54.032	0.684
	60	31.046	0.600
	70	59.002	0.683
	80	53.117	0.660

Table 3. Detonation tube $R(m) = A[t(s)]^n$: space-time diagrams coefficients of shock wave

Gaseous mixture	d (mm)	A	n
$C_3H_8 + 3O_2$	16	42.179	0.672
	26	49.227	0.675
	36	56.172	0.683
$C_3H_8 + 5O_2$	16	41.355	0.673
	26	50.391	0.681
	36	57.817	0.682
$C_3H_8 + 7O_2$	16	46.196	0.690
	26	51.932	0.687
	36	56.406	0.686
$C_3H_8 + 0.5O_2$	16	49.271	0.706

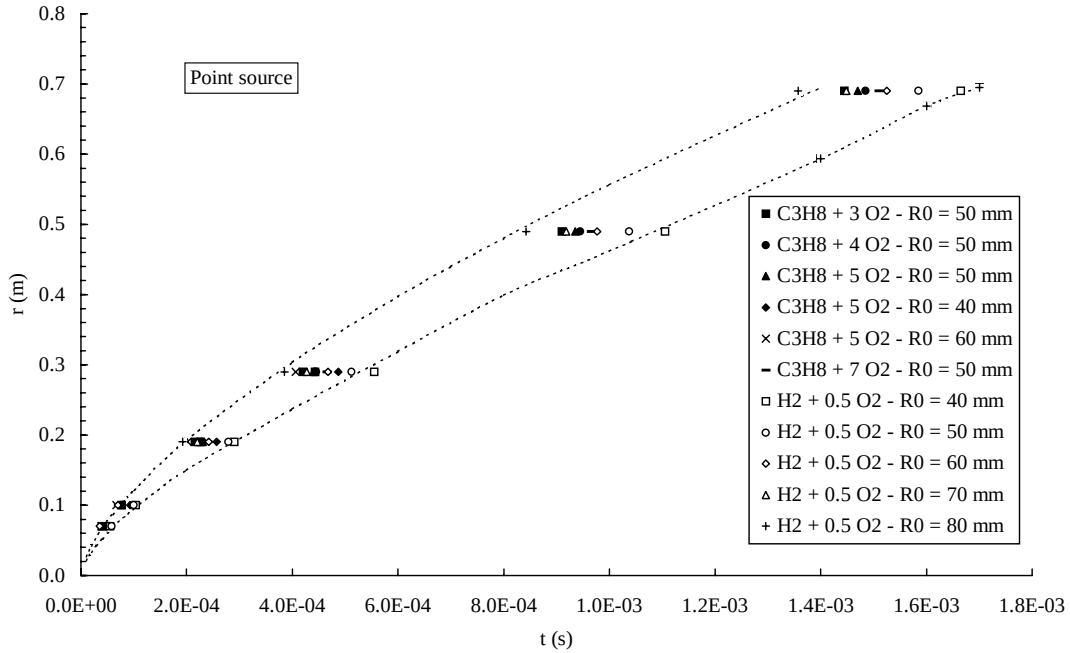

Fig. 4. Space-time diagram of shock wave: point source

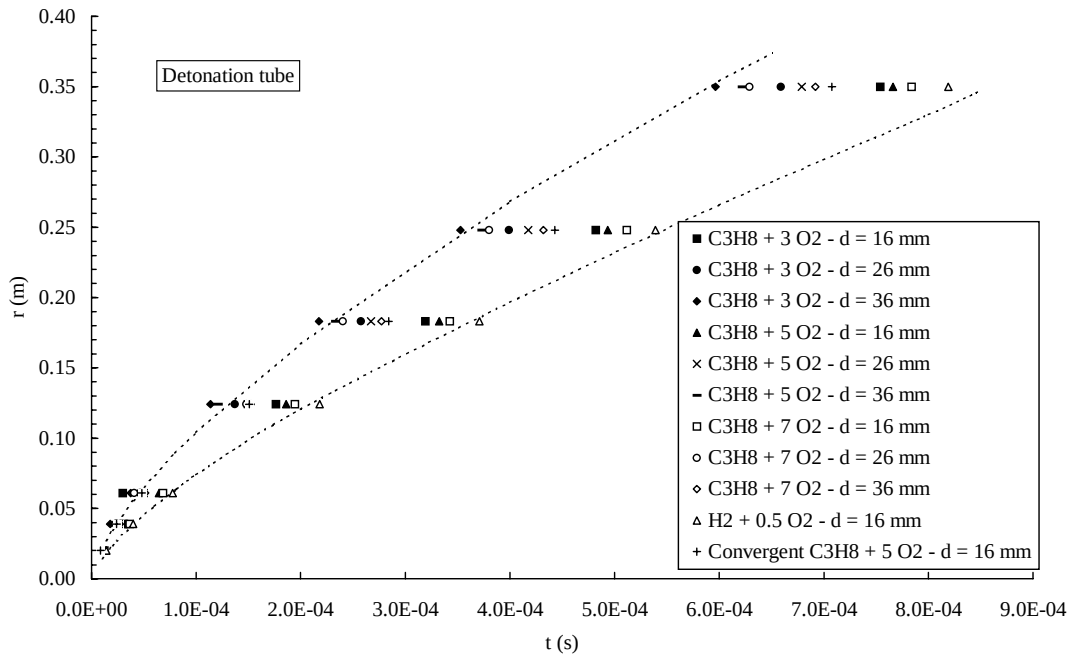

Fig. 5. Space-time diagram of shock wave: detonation tube

$r \propto 300$ mm and $4.5 \times 10^{-4} \leq t(s) \leq 6.7 \times 10^{-4}$ for the detonation tube. Although the two space-time (Figs. 4, 5) and pressure-space (Figs. 6, 7) diagrams were obtained independently, in fact, they represent the same physical phenomenon. A velocity is associated at each point of $(r-t)$ diagram. Hence, the intensity p/p_0 of shock wave can be calculated: the result being a point on the pressure-space $(p-r)$ diagram. Consequently, there is a correlation between the two diagrams. At the origin ($r = 0$) the law $r = At^n$ results in a zero velocity which is incompatible with the observed intensity on the pressure-space diagram: p/p_0 has a finite non zero value. To give compatibility between the families of diagrams, an imaginary center of explosion (r^*, t^*) is introduced. This imaginary center (r^*, t^*) of explosion is defined by $(r + r^*) = A(t + t^*)^n$ such as for $r = 0$, the velocity (i.e. the Mach number M) is con-

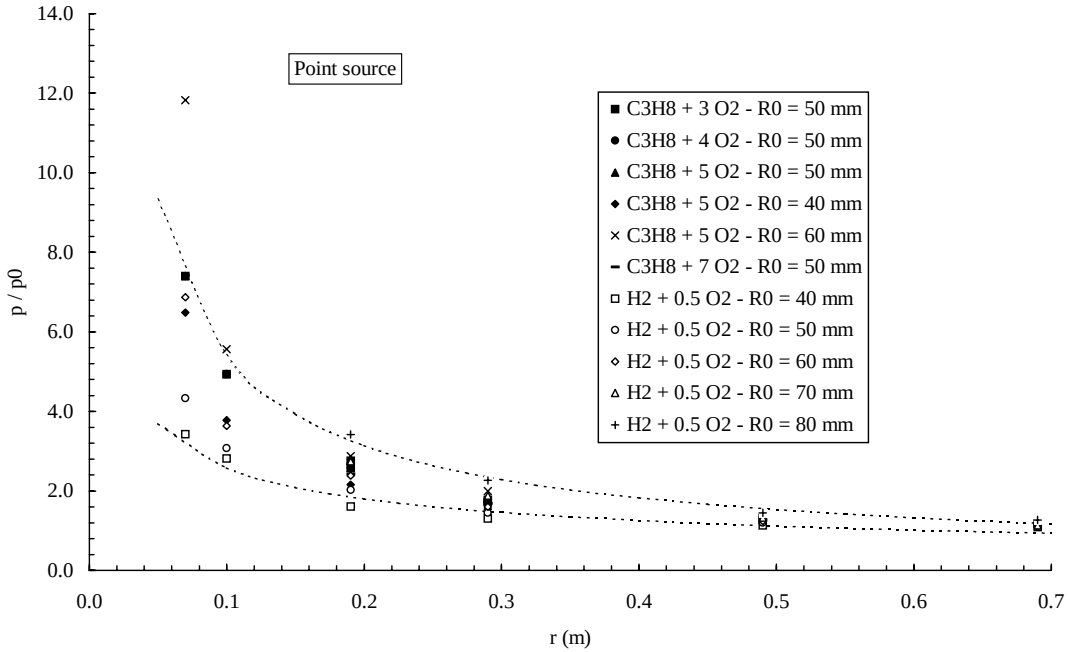

Fig. 6. Pressure-space diagram of shock wave: point source

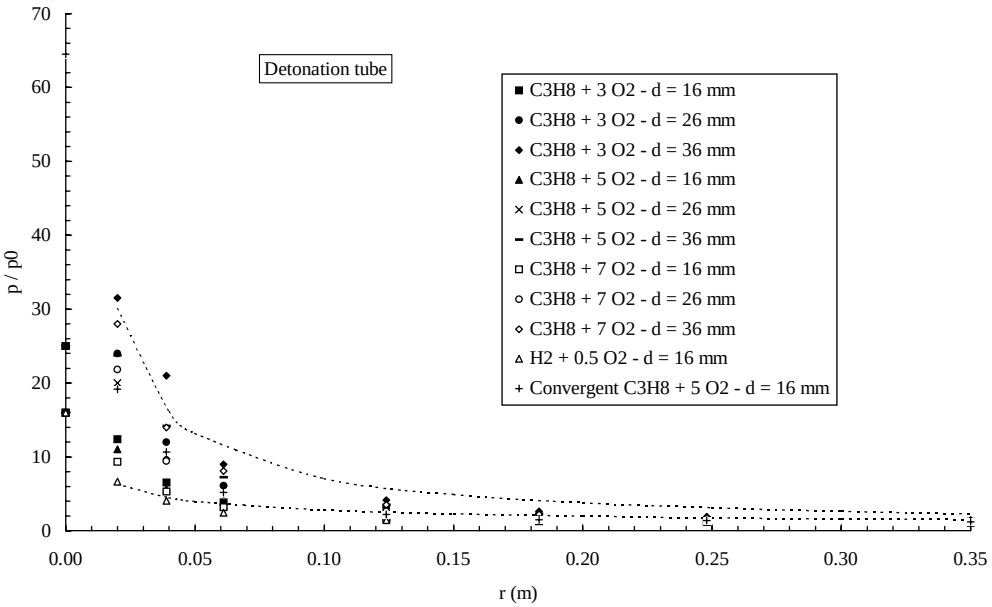

Fig. 7. Pressure-space diagram of shock wave: detonation tube

sistent with the intensity of shock wave $p(M)$. For that, two conditions must be verified : $\frac{d(r+r^*)}{dt} = nA(t+t^*)^{n-1}$ and especially if $r = 0$ and $t = 0$ then $r^* = At^{*n}$.

The variety of experimental results requires that one presents the radial distance of the shock front and the associated time in dimensionless variables. The shock radius is non-dimensionalyzed by the characteristic explosion length $(E/p_0)^{1/3}$ (spherical symmetry), where E is the energy as defined above and p_0 the ambient air pressure. The time is non-dimensionalyzed by $(E/p_0)^{1/3}/a_0$, where a_0 is the sound speed in ambient air. Hence, the dimensionless radial distance R and time T can be defined by the following relationships: $R = r/(E/p_0)^{1/3}$ and $T = a_0 t/(E/p_0)^{1/3}$.

As mentioned earlier, r and t can be corrected. The transformation of (r, t) into $(r + r^*, t + t^*)$ does not modify the following analysis. In fact, (r^*, t^*) is very small compared with the measurements scale. (So, the contribu-

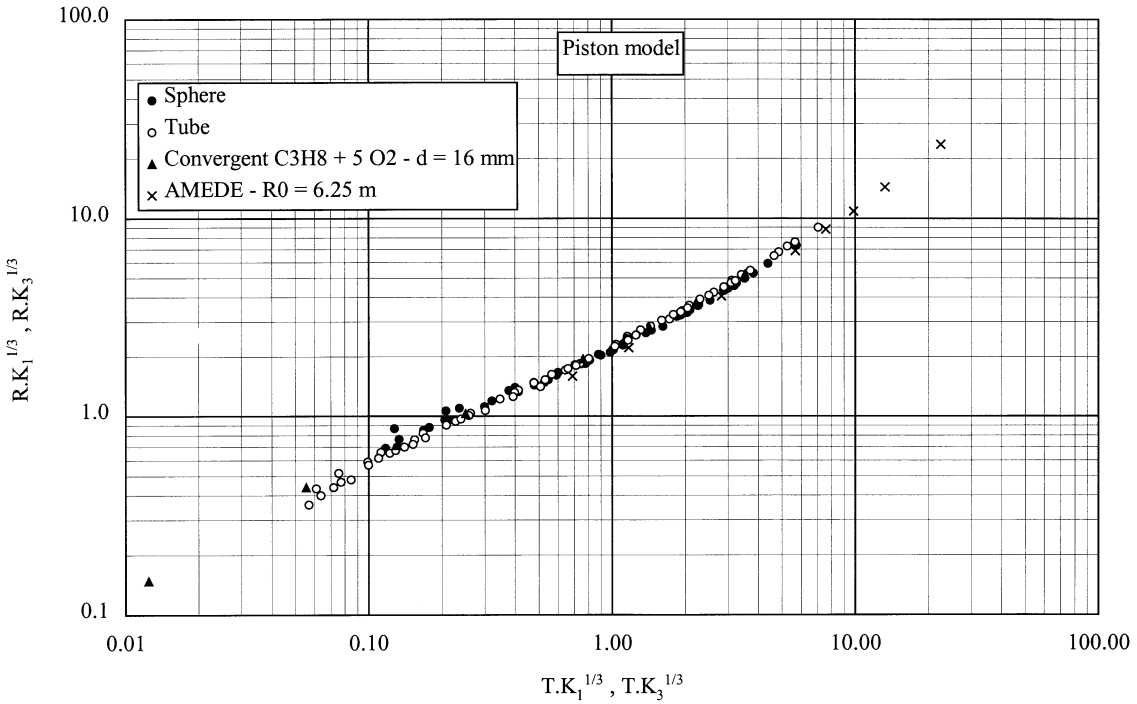

Fig. 8. Dimensionless space-time diagram of shock wave, piston model

tion to the energy quantification is of little significance). The dimensionless pressure is noted by $P = p/p_0$, which represents the ratio of the maximum pressure p over the ambient air pressure p_0.

4.3 Comparison with other explosions

We have expressed all of our experimental results in dimensionless variables (R, T, P) using both formulations of energy. However, the constants $(K_i,\ i = 1, 2, 3, 4)$ in the expression of energy must be evaluated. Thus we present the dimensionless diagrams in a form independent of the constants. The dimensionless space-time $(R.K_i^{1/3}, T.K_i^{1/3})$ (Figs. 8, 9) and pressure-space $(P, R.K_i^{1/3})$ (Figs. 10, 11) diagrams show that there is a perfect correlation between the different gaseous mixtures and volumes of hemispherical confinement on the one hand and the diameters of tube on the other (propagation direction corresponds to the tube axis). The results obtained with the tube utilizing the convergent section superpose on the other results and extend the range of the results.

In addition, we introduce experiments of different authors into the diagrams. The AMEDE experiments (Brossard (1982) used large-scale explosions. We report an example of trials in this analysis. A mixture of ethylene/air is confined in a hemispherical volume ($R_0 = 6.25$ m) and is initiated by a small charge of solid explosive. The AMEDE results (Figs. 8, 9, 11) are in good agreement with our small-scale experiments, and allow their continuation to large distances.

With regard to the pressure-space diagram (P, R) (Fig. 11) of the blast effect from gaseous explosion Dorofeev (1996) calculates the following expression:

$$\Delta p^+/p_0 = (0.34/R^{4/3}) + (0.062/R^2) + (0.033/R^3), \quad (13)$$

while Desrosier et al. (1991) expresses experimental results in the following least-square polynomial form:

$$\ln(\Delta p^+/p_0) = 0.299 - 2.058 \ln (rE^{-1/3}) + 0.260(\ln(rE^{-1/3}))^2, \quad (14)$$

where, E is the chemical energy released in the volume of $4\pi R_0^3/3$.

5 Discussion

We summarize here the relationships for the different considered cases:

$$R = \frac{r}{(E/p_0)^{1/3}}, \qquad T = \frac{a_0 t}{(E/p_0)^{1/3}}, \qquad P = \frac{p}{p_0},$$

for a blast wave resulting of the explosion of a spherical charge of initial radius R_0: (i) piston model: $E = K_3 p \frac{u}{a} R_0^3$; (ii) volumic energy model: $E = K_4 E_v R_0^3$, while for a planar detonation or shock wave propagating in a tube of diameter d and emerging into unconfined air environment we find: (i) piston model:$E = K_1 p \frac{u}{a} d^3$; (ii) volumic energy model: $E = K_2 E_v d^3$, where p, u, a denote the pressure, the particle velocity and sound speed, respectively, downstream the shock or the detonation wave. E_v represents

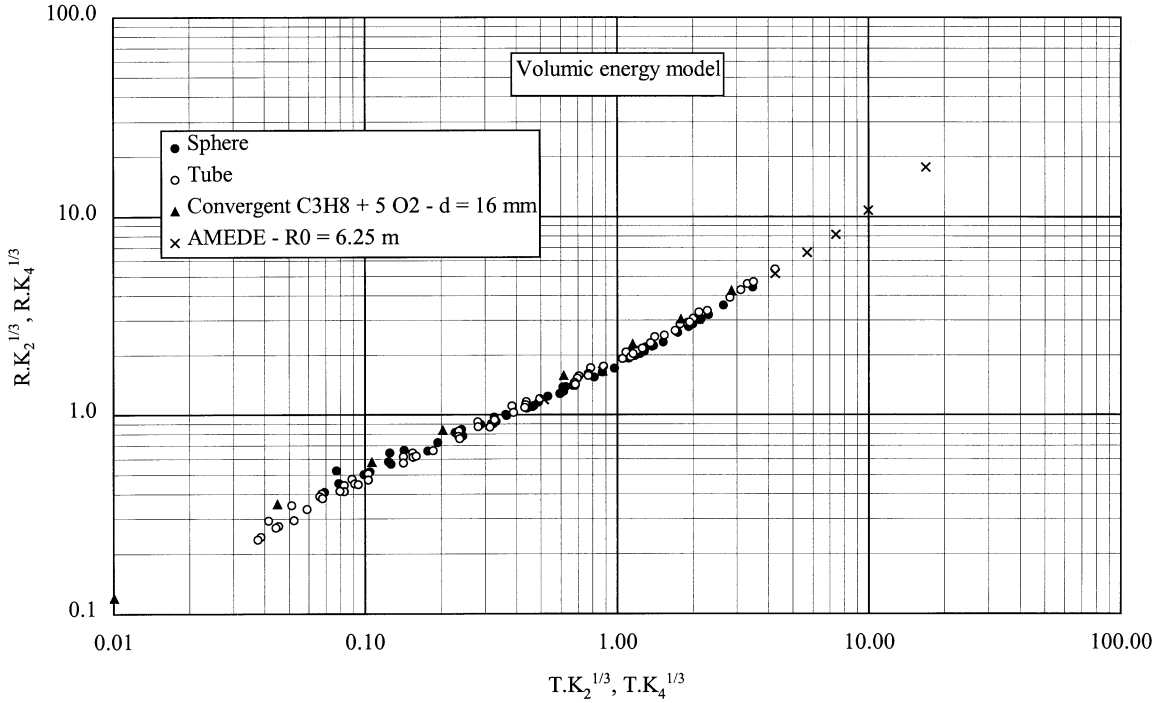

Fig. 9. Dimensionless space-time diagram of shock wave - bulk energy model

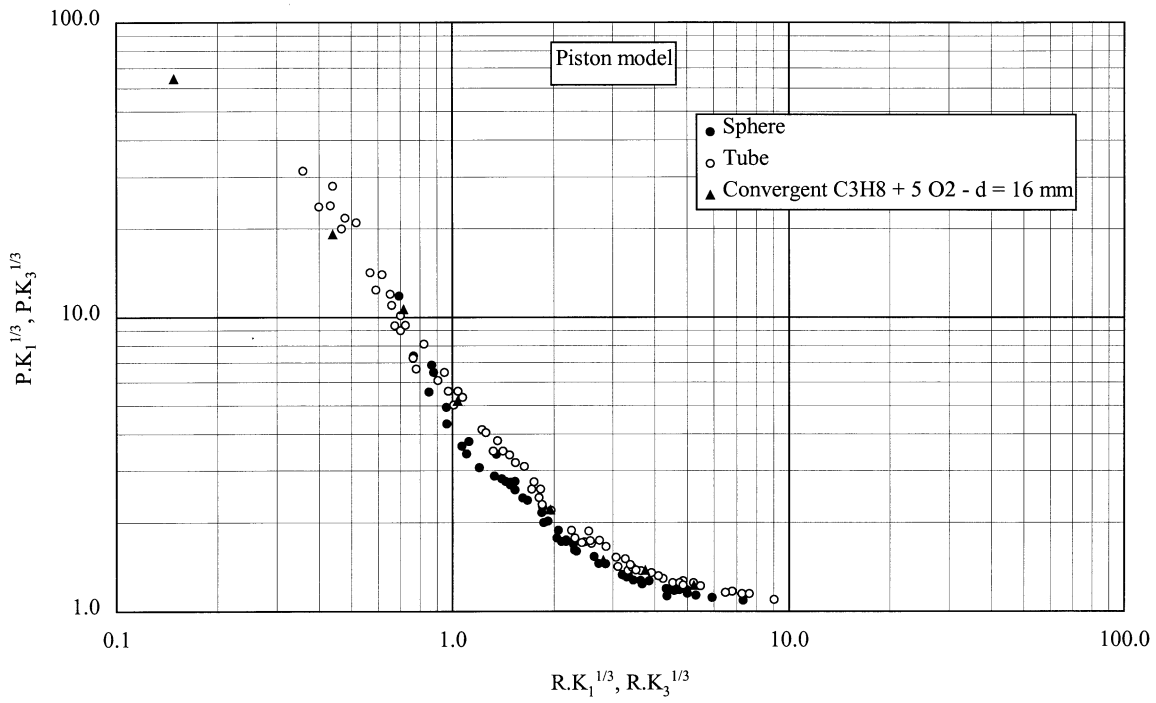

Fig. 10. Dimensionless pressure-space diagram of shock wave – piston model

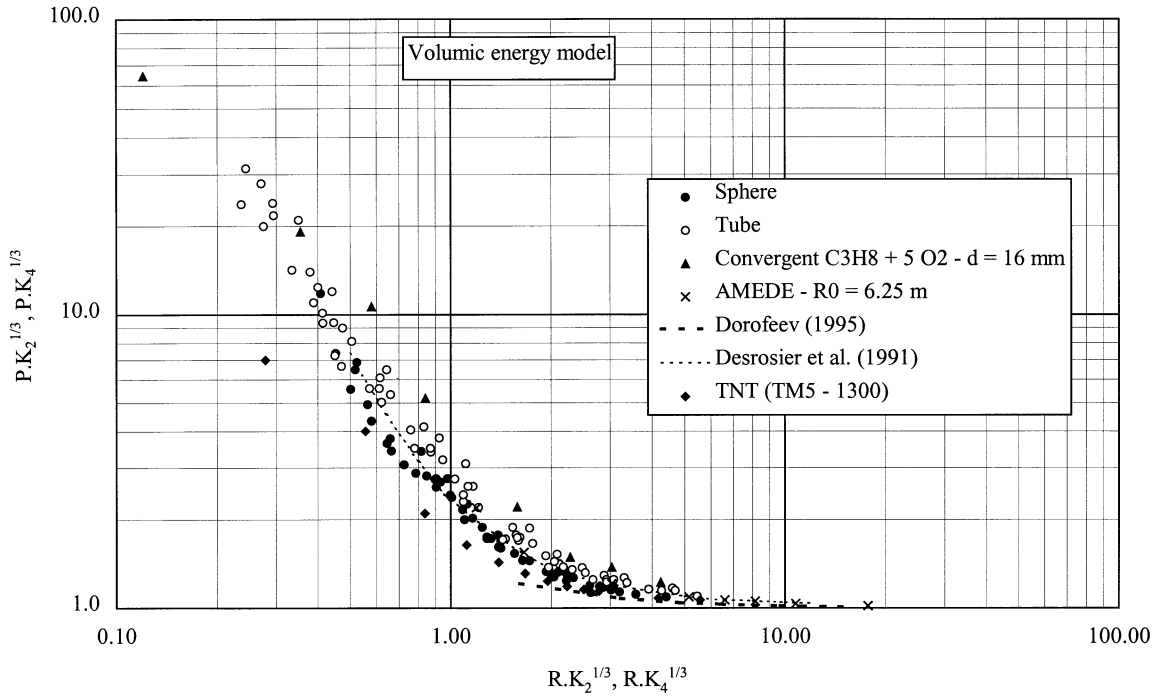

Fig. 11. Dimensionless pressure-space diagram of shock wave – volumic energy model

the chemical energy per unit volume released by the reaction or the sum of kinetic and internal energies of the gas bounded by the shock wave.

The two series of diagrams space-time: (r,t) and pressure-range: (p,r), correspond to the same physical phenomenon. Consequently, there are two ways to express the energy in the dimensionless approach: (i) a correspondence of reduced parameters, and (ii) evaluation of the constants. The identification of parameters is conducted:

(1) By comparison of curves for a given dimensionless diagram. The results obtained in different cases (Figs. 8, 9, 10, 11) can be identified to a one-curve. Hence, the following quasi-equalities can be defined: for the piston model (Figs. 8, 10) $R_0 \simeq d$ and $K_3 = K_1$, while for the volumic energy model (Figs. 9, 11) $R_0 \simeq d$ and $K_4 = K_2$.
(2) By translation parallel to the first bisecting line of one curve pattern on the other for the dimensionless diagram $(r-t)$, or by translation parallel to the abscissa axis for the dimensionless diagram $(p-r)$. We note that the two translations result in the same equivalency:

$$\left(\frac{K_3}{K_4}\right)^{1/3} = \left(\frac{K_1}{K_2}\right)^{1/3} = 0.6.$$

For waves coincident with a spherical explosion, it is clear that $K_4 = 4\pi/3$, and as a consequence the other constants (K_3, K_2 and K_1) can be quantified: $K_4 = K_2 = \frac{4}{3}\pi$ and $K_3 = K_1 = \frac{\pi}{3.47}$ Finally, the energy source formulations are given by:

$$E = \frac{\pi}{3.47} p \frac{u}{a} d^3, \tag{15}$$

or

$$E = \frac{\pi}{3.47} p \frac{u}{a} R_0^3 \tag{16}$$

for the piston model, and by:

$$E = \frac{4}{3}\pi E_v d^3, \tag{17}$$

or

$$E = \frac{4}{3}\pi E_v R_0^3 \tag{18}$$

for the bulk energy model.

We note that the constant K_3 differs from the constant proposed by Matsui and Lee (1979) or by Desbordes (1988). However, these energy formulations allow us to calculate the energy supplied either by a planar detonation or shock wave propagating in a tube of diameter d and emerging into unconfined air environment (13, 15) or by a blast wave resulting of the explosion of a spherical charge of initial radius R_0 (14, 16). However, these energy formulations do not allow us to calculate the minimal energy to initiate a spherical detonation. For engineering applications, it is important to be able to predict the critical initiation energy of spherical detonation. We then ask the following question: under critical conditions, is the energy released by planar detonation equal to the ignition source energy supply? Given that from an experimental point of view: in case of the confined planar detonation wave transmission at the open end of a tube into an unconfined environment, the critical diameter is an easily measured parameter; in case of a point source, the critical initiation energy is the accessible variable (if the efficiency of the

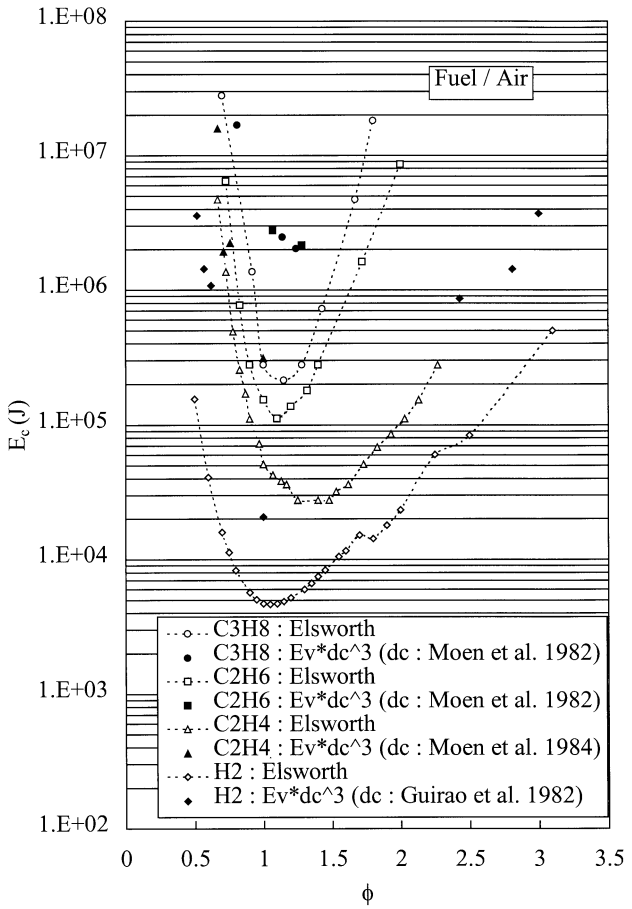

Fig. 12. Critical energy versus equivalence ratio – $p_0 = 1$ atm $- T_0 = 298$ K

igniter source is known then the critical energy is a critical efficiency energy else it is a critical nominal energy). This is why, by analogy with previous energy formulations, we propose to correlate the initiation energy of a point source with the group of terms $E_v d_c^3$. For that and from only experimental results, we plot (Fig. 12) the direct critical initiation energy and the product $E_v d_c^3$ versus the equivalence ratio relative to different fuel/air mixtures. To our knowledge unfortunately, no similar experimental data of critical energies and critical diameter have been reported for fuel/oxygen mixtures: the bulk of results are predicted by theoretical models. We use Elsworth's unpublished work reported by Benedick et al. (1986). The comparison of the data means that it is possible to slide data points of direct initiation on representative points of $E_v d_c^3$. In the range of considered fuel in this work, a correlation coefficient 0.06 as a rough average value can be adopted, then: E for initiation point source is,

$$E = 0.06 E_v d_c^3. \tag{19}$$

Consequently, we answer to the question: under critical conditions, there is a correlation between the two types of initiation energy.

Under these conditions, we can approach another important problem of the detonation theory, which can be formulated by the following question: is it possible to link the critical tube diameter d_c to the critical radius of detonation R_{cCJ}. The critical radius of detonation R_{cCJ} corresponds to the minimum propagation distance of the flame front shock wave complex for which CJ conditions are realized and defines the critical initiation energy of spherical detonation (Sochet et al, 1997):

$$E_c = \frac{4}{3}\pi E_v (3\Delta R_{cCJ}^2 - 3\Delta^2 R_{cCJ} + \Delta^3), \tag{20}$$

where Δ is the induction length.

For a given mixture, if we suppose (19) as being general, the comparison with (20) leads to:

$$\frac{4}{3}\pi E_v (3\Delta R_{cCJ}^2 - 3\Delta^2 R_{cCJ} + \Delta^3) = 0.06 E_v d_c^3. \tag{21}$$

The induction length Δ is very small compared to the critical radius of detonation R_{cCJ}, so under this condition (19) can be approximated by the following equation:

$$R_{cCJ} \approx 0.07 \left(\frac{d_c^3}{\Delta}\right)^{1/2} \quad \text{or} \quad \frac{R_{cCJ}}{d_c} = 0.07 \left(\frac{d_c}{\Delta}\right)^{1/2}. \tag{22}$$

This relationship between the critical radius of detonation R_{cCJ} and the critical tube diameter d_c does not require the knowledge of the cellular structure characteristics of the detonation wave. The induction length Δ can be calculated by a chemical kinetic model. Applications of this equation are presented in Table 4 for several stoichiometric fuel/oxygen and fuel/air mixtures. As may be seen the ratio R_{cCJ}/d_c can not be assimilated to a constant. The mean value of the ratio R_{cCJ}/d_c is 1.37 for fuel-oxygen mixtures. Unlike the approximation which could be conducted taking into account classical relations: $d_c = 13\lambda$ and $R_{cCJ} = 20\lambda$, in which λ represents the cell width, such as: $R_{cCJ}/d_c \approx 1.54$, similar to the previous value.

We note too that there is a second interest of the link between two types of critical initiation energy and the link between critical radius of detonation R_{cCJ} and the critical tube diameter d_c. Effectively, they enable one to define a critical initial volume or radius (noted by R_{oc}) of gaseous mixture under which no detonation can be obtained. This critical initial radius R_{oc} is deduced by the equality between the critical initiation energy (20) and (18) applied for critical conditions R_{cCJ} as follows:

$$\frac{4}{3}\pi E_v (3\Delta R_{cCJ}^2 - 3\Delta^2 R_{cCJ} + \Delta^3) = \frac{4}{3}\pi E_v R_{0c}^3. \tag{23}$$

Applying the assumption $\Delta << R_{cCJ}$, it can be deduced:

$$R_{0c} = (3\Delta R_{cCJ}^2)^{1/3} \text{ or } \frac{R_{0c}}{R_{cCJ}} = \left(3\frac{\Delta}{R_{cCJ}}\right)^{1/3}. \tag{24}$$

It turns out that the ratio R_{0c}/R_{cCJ} is in order of 0.2 (Table 4).

Table 4. Calculated critical energy of detonation for stoichiometric mixtures - $p_0 = 1$ atm - $T_0 = 298$ K

Fuel / Oxygen	d_c (m)	Δ (m)	R_{cCJ} (m)	R_{cCJ}/d_c	R_{0c} (m)	R_{0c}/R_{cCJ}
H_2	0.020	44.9×10^{-6}	0.029	1.48	0.005	0.16
CH_4	0.053	133.0×10^{-6}	0.074	1.40	0.013	0.17
C_2H_4	0.006	28.2×10^{-6}	0.006	1.02	0.001	0.24
C_2H_6	0.015	37.8×10^{-6}	0.021	1.39	0.004	0.17
C_3H_8	0.012	24×10^{-6}	0.019	1.56	0.003	0.16

d_c: Matsui and Lee (1979) Δ: H_2, CH_4, C_2H_4, C_2H_6, Westbrook and Urtiew (1982); C_3H_8, Westbrook et al. (1984)

Fuel / Air	d_c (m)	Δ (m)	R_{cCJ} (m)	R_{cCJ}	R_{0c} (m)	R_{cCJ}
H_2	0.200	0.287×10-3	0.37	1.85	0.05	0.13
CH_4	0.115	0.273×10-3	0.16	1.44	0.03	0.17
C_2H_4	0.430	2.560×10-3	0.39	0.91	0.10	0.27
C_2H_6	0.900	4.550×10-3	0.88	0.98	0.22	0.25
C_3H_8	0.900	4.510×10-3	0.89	0.99	0.22	0.25

d_c: Moen et al. (1982) Δ: H_2, CH_4, C_2H_4, C_2H_6, Westbrook and Urtiew (1982); C_3H_8, Westbrook et al. (1984)

6 Conclusion

Dimensional analysis demonstrates the similarity of blast waves generated by a spherical gaseous detonation, and a planar detonation emerging from a tube. The energy released by the planar detonation tube is comparable to the initiation energy of a spherical detonation. Energy formulations are obtained from the analogy of the two types of initiation. By this analogy, we show that under critical conditions, the ignition source energy supply is proportional to the energy released by planar detonation, if this last one is represented by the term $E_v d_c^3$. This proportionality allows: (i) to establish a link between critical radius of detonation R_{cCJ} and the critical tube diameter d_c; (ii) to quantify a critical initial radius R_{oc} of gaseous mixture under which no detonation can be obtained with a critical initiation energy.

References

Benedick WB, Guirao CH, Knystautas R, Lee JH (1986) Critical charge for the direct initiation of detonation in gaseous fuel-air mixtures. Dynamics of Explosions, Prog in Astro Aero AIAA 106: 181-202

Brossard J (1982) Les Essais AMEDE 2/8 et Premiers resultats de synthèse. Note EA. 79/15

Desbordes D (1988) Transmission of overdriven plane detonations: critical diameter as a function of cell regularity and size. Prog in Astro Aero, AIAA, 11: 170-185

Desrosier C, Reboux A, Brossard J (1991) Effect of Asymmetric ignition on the vapor cloud spatial blast. Dynamics of Detonations and Explosions, Prog in Astro Aero AIAA, 134: 21-37

Dorofeev SB (1996) Blast effects of confined and unconfined explosions. Proc of the 20th Int Symp on Shock Waves I: 77-86

Guiaro CM, Knystautas R, Lee JH, Benedick WB, Berman M (1982) Hydrogen-air detonation. In: XIXth Int Symp on Comb, The Combustion Institute,Pittsburgh, pp. 583-590

Lee JH (1984) Dynamic parameters of gaseous detonations. Ann Rev Fluid Mech, 16: 311-336

Matsui H, Lee JH (1979) On the measure of the Relative Detonation Hazards of Gaseous Fuel-Oxygen Mixtures. XVIIth Int Symp on Comb, The Combustion Institute,Pittsburgh, pp. 1269-1278

Moen IO, Funk JW, Ward SA, Rude GM, Thibault PA (1984) Detonation length scales for fuel-air explosives. Dynamics of Shock Waves: Explo and Deto, Progress in Astro Aero AIAA, 94: 55-79

Moen IO, Murray SB, Bjerketvedt D, Rinnan A, Knystautas R, Lee JH (1982) Diffraction of detonation from tubes into a large fuel-air explosive cloud. In: XIXth Int Symp on Comb, The Combustion Institute,Pittsburgh, pp. 635-644

Sedov L (1977) Similitude et dimensions en mécanique. Traduction Française, éditions Mir, Moscou

Sochet I, Reboux A, Brossard J (1993) Detonability of spatially non-uniform gaseous mixtures. In: 14th Int Col on Dynamics of Explo and Reactive Systems, Proceedings II: E.1.7.1-E.1.7.10

Sochet I, Aminallah M, Brossard J (1997) Detonability of fuel-oxygen and fuel-air mixtures. Shock Waves 7: 163-174

Westbrook CK, Urtiew PA (1982) Chemical Kinetics Prediction of Critical Parameters in Gaseous Detonations. In: XIXth Int Symp on Comb, The Combustion Institute,Pittsburgh, pp. 615-623

Westbrook CK, Pitz WJ, Urtiew PA (1984) Chemical Kinetics of Propane Oxidation in Gaseous Detonations. In: Dynamics of Shock Waves: Explo and Deto, Progress in Astro Aero AIAA, 94: 151-174